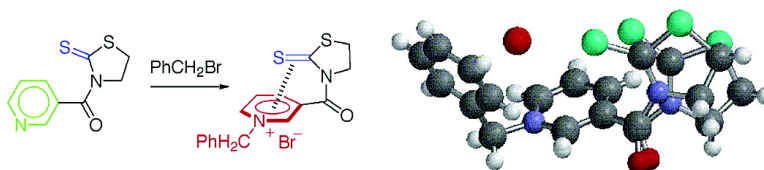Article

Cation–ꙮ Interactions of a Thiocarbonyl Group and a Carbonyl Group with a Pyridinium Nucleus

Shinji Yamada, Tomoko Misono, and Seiji Tsuzuki

More About This Article

Additional resources and features associated with this article are available within the HTML version:

- Supporting Information
- Links to the 3 articles that cite this article, as of the time of this article download
- Access to high resolution figures
- Links to articles and content related to this article
- Copyright permission to reproduce figures and/or text from this article

View the Full Text HTML

Cation−π Interactions of a Thiocarbonyl Group and a Carbonyl Group with a Pyridinium Nucleus

Shinji Yamada,*,† Tomoko Misono,† and Seiji Tsuzuki‡

Contribution from Department of Chemistry, Faculty of Science, Ochanomizu University, Bunkyo-ku, Tokyo 112-8610, Japan and National Institute of Advanced Industrial Science and Technology, Tsukuba, Ibaraki 305-8568, Japan

Received February 21, 2004; E-mail: yamada@cc.ocha.ac.jp

Abstract: Attractive interactions between a thiocarbonyl group and a pyridinium nucleus, and between a carbonyl group and a pyridinium nucleus have been proven by ^{1}H and ^{13}C NMR studies, UV−vis spectral analyses, and X-ray crystallographic analyses of nicotinic amides **1** and **3**, and pyridinium salts **2** and **4**. Comparison of the $\Delta\delta$ values, which are the differences in the chemical shifts with reference compounds **5** or **6**, showed that the absolute $\Delta\delta$ values of **2** and **4** are much larger than those of **1** and **3**. In the UV−vis spectra, the $n{\rightarrow}\pi^*$ absorption of the C=S group of **2a** exhibited a significant blue shift in CHCl₃. X-ray crystallographic analysis of **1**−**4** clearly showed that the C=S group of **2a** and the C=O group of **4** are very close to the pyridinium moiety compared to the case of **1** and **3**. In addition, the X-ray crystal packing structure of **2a** showed the C=S group is sandwiched between two pyridinium rings. These experimental results strongly suggested the existence of attractive (C=S)···Py⁺ and (C=O)···Py⁺ interactions in solution and in crystal. The optimized geometries of **1** and **2** calculated at the HF/6-311G** level are in good agreement with their X-ray geometries. MP2/6-311G** calculations for the model systems of pyridinium salts **2** and **4** predicted that the electrostatic and induction energies are the major source of the attractive interactions. Since the larger contribution of electrostatic and induction interactions are characteristic features of cation−π interactions, the (C=S)···Py⁺ and (C=O)···Py⁺ interactions would be classified as a cation−π interaction.

Introduction

The significant importance of the cation−π interactions in conformation control and molecular recognition has been well documented in recent numerous literature.[1] In particular, the cation−π interactions play a key role in the construction of inclusion complexes[2] and protein structures[3] as well as in biological recognitions.[4] In addition, the conformation-controlling ability has opened up new methods for the stereoselective synthesis.[5,6] Although most of the reported cation−π interactions are observed between a cationic moiety and an aromatic π-component, little is known about nonaromatic π-systems except for the complexes of ethylene−ammonium cation[7] and acetylene−Ca⁺.[8] Therefore, disclosure of a new type of cation−π interaction would be of significant interest.

During our studies on the faceselective addition of nucleophiles to pyridinium salts bearing a 1,3-thiazolidine-2-thione moiety,[9] we presumed that the resulted face-selectivities are attributable to the conformational rigidity arising from an intramolecular interaction between the pyridinium ring and the thiocarbonyl group.[10] The shielding of one face of the pyridinium ring with the thiocarbonyl group enables nucleophiles to attack from the nonshielding face as shown in Scheme 1. Although there have been known various types of nonbonding intra- and intermolecular interactions involving a sulfur atom such as S···N,[11] S···O,[12] S···S,[13] and S···π[14] interactions, this

† Department of Chemistry, Faculty of Science, Ochanomizu University.
‡ National Institute of Advanced Industrial Science and Technology.

(1) For reviews, see: (a) Meyer, E. A.; Castellano, R. K.; Diederich, F. *Angew. Chem., Int. Ed.* **2003**, *42*, 1210−1250. (b) Gokel, G. W.; De Wall, S. L.; Meadows, E. S. *Eur. J. Org. Chem.* **2000**, 2967−2978. (c) Ma, J. C.; Dougherty, D. A. *Chem. Rev.* **1997**, *97*, 1303−1324. (d) Dougherty, D. A. *Science* **1996**, *271*, 163−168.

(2) (a) Gokel, G. W.; Barbour, L. J.; Ferdani, R.; Hu, J. *Acc. Chem. Res.* **2002**, *35*, 878−886. (b) Abraham, W. *J. Inclusion Phenom. Macrocyc. Chem.* **2002**, *43*, 159−174. (c) Gokel, G. W.; Barbour, L. J.; De Wall, S. L.; Meadows, E. S. *Coord. Chem. Rev.* **2001**, *222*, 127−154. (d) Ferdani, R.; Hu, J.; Leevy, W. M.; Pajewska, J.; Pajewski, R.; Villalobos, V.; Barbour, L. J.; Gokel, G. W. *J. Inclusion Phenom. Macrocyc. Chem.* **2001**, *41*, 7−12. (e) Shinkai, S.; Ikeda, A. *Pure Appl. Chem.* **1999**, *71*, 275−280. (f) Lhotak, P.; Shinkai, S. *J. Phy. Org. Chem.* **1997**, *10*, 273−285. (g) Araki, K. *Yuki Gosei Kagaku Kyokaishi* **1995**, *53*, 22−31.

(3) For reviews, see: (a) Shi, Z.; Olson, C. A.; Bell, A. J., Jr.; Kallenbach, N. R. *Biopolymers* **2001**, *60*, 366−380. (b) Moise, L.; Zeng, H.; Caffery, P.; Rogowski, R. S.; Hawrot, E. *J. Toxicol. Toxin Rev.* **2002**, *21*, 293−317.

(4) For reviews, see: (a) Zacharias, N.; Dougherty, D. A. *Trends Pharmacol. Sci.* **2002**, *23*, 281−287. (b) Watts, A. *Mol. Membrane Biol.* **2002**, *19*, 267−275. (c) Tonder, J. E.; Olesen, P. H. *Curr. Med. Chem.* **2001**, *8*, 651−674. (d) Schmitt, J. D. *Curr. Med. Chem.* **2000**, *7*, 749−800. (e) Scrutton, Nigel S.; Raine, Andrew R. C. *Biochem. J.* **1996**, *319*, 1−8.

(5) For a review, see: Ramamurthy, V.; Shailaja, J.; Kaanumalle, L. S.; Sunoj, R. B.; Chandrasekhar, J. *Chem. Commun.* **2003**, 1987−1999.

(6) (a) Katz, C. E.; Aubé, J. *J. Am. Chem. Soc.* **2003**, *125*, 13 948−13 949. (b) Yamada, S.; Morita, C. *J. Am. Chem. Soc.* **2002**, *124*, 8184−8185.

(7) Deakyne, C. A.; Meot-Ner (Mautner), M. *J. Am. Chem. Soc.* **1985**, *107*, 474−479.

(8) France, M. R.; Pullins, S. H.; Duncan, M. A. *J. Chem. Phys.* **1998**, *108*, 7049−7051.

(9) (a) Yamada, S.; Ichikawa, M. *Tetrahedron Lett.* **1999**, *40*, 4231−4234. (b) Yamada, S.; Morita, C. *Chem. Lett.* **2001**, 1034−1035. (c) Yamada, S.; Misono, T.; Ichikawa, M.; Morita, C. *Tetrahedron* **2001**, *57*, 8939−8949.

(10) Preliminary communication: Yamada, S.; Misono, T. *Tetrahedron Lett.* **2001**, *42*, 5497−5500.

(11) Ohkata, K.; Ohsugi, M.; Yamamoto, K.; Ohsawa, M.; Akiba, K.-y. *J. Am. Chem. Soc.* **1996**, *118*, 6355−6369, and references therein.

type of interaction has not yet been explored. Such nonbonding interactions have received considerable attention due to their essential roles in controlling the molecular conformation and molecular recognition in compounds containing a sulfur atom. Moreover, these interactions are interesting in relation to biological activity of various heterocyclic compounds.

In this paper we describe the existence of attractive intra- and intermolecular $(C=S)\cdots Py^+$ and $(C=O)\cdots Py^+$ interactions, which were elucidated by ^1H and ^{13}C NMR spectroscopy, UV–vis spectroscopy, and X-ray crystallographic analyses and ab initio calculations. Furthermore, the origin of the attraction is also estimated.

Scheme 1. Selective Addition Reaction by Way of $(C=S)\cdots Py^+$ Interaction
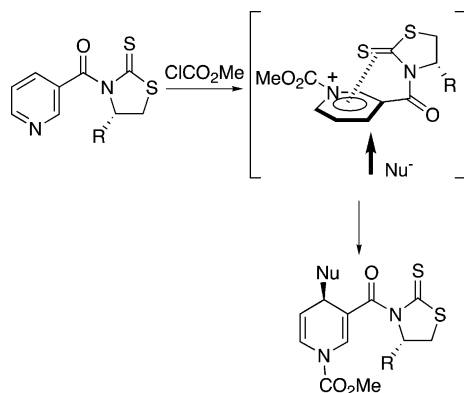
Results and Discussion

As substrates we employed pyridine derivatives **1**, **3**, and **5**, and the corresponding pyridinium salts **2**, **4**, and **6**. **1** and **2** have a 1,3-thiazolidine-2-thione group, and **3** and **4** have a 1,3-oxazolidine-2-one group, which were prepared according to the reported method.[9c] Nicotinic amide **5** and its salt **6**[9c] are reference compounds for ^1H and ^{13}C NMR studies. ^1H and ^{13}C NMR measurements of **1**–**6**, UV–vis measurements of **1** and **2a**, and X-ray crystallographic analyses of **1**, **2a**, **3** and **4** were carried out to investigate structural differences among **1**–**4**.
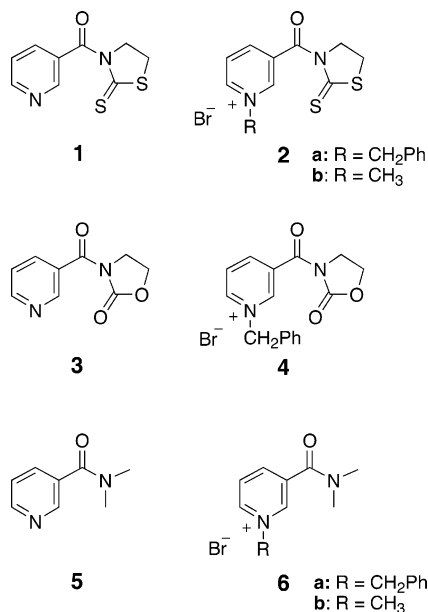

Table 1. ^1H NMR Chemical Shifts[a] of **1**–**6** and the $\Delta\delta$ Values[b] (ppm)

compd	solv	δ_{H2}	δ_{H4}	δ_{H5}	δ_{H6}	$\Delta\delta_{H2}$	$\Delta\delta_{H4}$	$\Delta\delta_{H5}$	$\Delta\delta_{H6}$
1	CDCl$_3$	8.87	7.95	7.35	8.71	0.19	0.17	-0.01	0.05
2a	CDCl$_3$	10.81	8.51	7.91	8.93	1.06	−0.06	−0.28	-0.86
2a	CD$_3$CN	9.48	8.61	8.08	8.93	-0.05	0.04	-0.06	-0.47
2a	DMSO-d_6	9.63	8.80	8.25	9.26	-0.01	0.05	-0.05	-0.20
2b	CDCl$_3$	10.72	8.57	7.99	8.71	1.57	0.12	-0.16	−0.64
2b	CD$_3$CN	9.15	8.61	8.02	8.72	0.30	0.14	-0.03	-0.06
2b	DMSO-d_6	9.42	8.79	8.19	9.07	0.22	0.16	0.01	0.02
3	CDCl$_3$	8.87	7.95	7.38	8.75	0.19	0.17	0.02	0.09
4	CDCl$_3$	10.43	8.63	8.01	9.33	0.64	0.06	-0.18	-0.42
4	CD$_3$CN	9.29	8.64	8.10	8.98	-0.03	0.11	-0.08	-0.24
4	DMSO-d_6	9.63	8.83	8.29	9.36	-0.01	0.08	-0.01	-0.10
5	CDCl$_3$	8.68	7.78	7.36	8.66				
6a	CDCl$_3$	9.75	8.57	8.19	9.79				
	CD$_3$CN	9.53	8.57	8.14	9.40				
	DMSO-d_6	9.64	8.75	8.30	9.46				
6b	CDCl$_3$	9.15	8.45	8.15	9.35				
	CD$_3$CN	8.85	8.47	8.05	8.78				
	DMSO-d_6	9.20	8.63	8.18	9.05				

[a] ^1H NMR chemical shifts are measured at 400 MHz. [b] $\Delta\delta = \delta 2 - \delta 1$ or $\delta 4 - \delta 3$.

^1H and ^{13}C NMR Studies. ^1H and ^{13}C NMR measurements of **1** – **6** were carried out in CDCl$_3$, CD$_3$CN, and DMSO-d_6 at r.t. Table 1 shows the ^1H NMR chemical shifts of the pyridine and the pyridinium protons, and the $\Delta\delta$ values that are the differences in the chemical shifts of **1** or **3** with standard **5**, and those of **2** or **4** with standard **6**. All of the $\Delta\delta$ values for neutral pyridine derivatives **1** and **3** are very small, whereas the $\Delta\delta$ values for the pyridinium salts **2a**, **2b**, and **4** are significantly dependent on the pyridinium protons.

Remarkable is that $\Delta\delta_{H2}$ for **2a** and **2b** in CDCl$_3$ are very large (1.06 and 1.57, respectively), whereas $\Delta\delta_{H6}$ are negatively very large (−0.86 and −0.64, respectively). On the other hand, the $\Delta\delta_{H4}$ and $\Delta\delta_{H5}$ are much smaller than the absolute values of $\Delta\delta_{H2}$ and $\Delta\delta_{H6}$. A similar trend was also seen in **4**, though the absolute $\Delta\delta$ values were smaller than those of **2a** and **2b**. It has to be noted that a magnetic anisotropic effect of the *N*-benzyl moiety is not responsible for the unusual downfield shift of H2 and upfield shift of H6 because the ^1H NMR behavior of *N*-methyl salt **2b** closely resembles that of **2a** and **4**. Another characteristic feature is the significant solvent effects on the $\Delta\delta$ values; as the solvent polarity increases, the absolute values of $\Delta\delta_{H2}$ and $\Delta\delta_{H6}$ decreased.

Figure 1 displays the plots of the $\Delta\delta$ values of **2a** and **4** for the pyridinium protons. This clearly shows the profiles of the $\Delta\delta$ values between **2a** and **4** to be very close to each other: large $\Delta\delta_{H2}$, negatively large $\Delta\delta_{H6}$ in CDCl$_3$ and significant solvent dependence. The fact that such phenomenon is observed only in the pyridinium salts **2** and **4** having a positive charge strongly suggests the existence of an intramolecular interaction between the C=S or the C=O group with the pyridinium ring in CDCl$_3$. It is also apparent that the $\Delta\delta$ values of salts **2a** and **2b** are larger than those of **4**, indicating a stronger effect of the C=S group than of the C=O group on the $\Delta\delta$ values of the pyridinium protons.

(12) (a) Minyaev, R. M.; Minkin, V. I. *Can. J. Chem*. **1998**, *76*, 776−788. (b) Nagao, Y.; Hirata, T.; Goto, S.; Sano, S.; Kakehi, A.; Iizuka, K.; Shiro, M. *J. Am. Chem. Soc*. **1998**, *120*, 3104−3110, and references therein.
(13) (a) Nagao, Y.; Nishijima, H.; Iimori, H.; Ushirogochi, H.; Sano, S.; Shiro, J. *J. Organometallic Chem*. **2000**, *611*, 172−177. (b) Rovira, C.; Novoa, J. J. *Chem. Eur. J*. **1999**, *5*, 3689−3697. (c) Wudl, F.; Srdanov, G.; Rosenau, B.; Wellman, D.; Williams, K.; Cox, S. D. *J. Am. Chem. Soc*. **1988**, *110*, 1316−1318, and references therein.
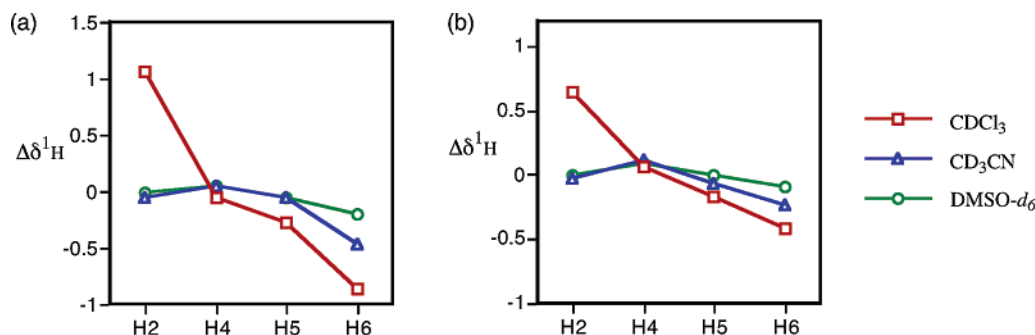
Figure 1. Plots of $\Delta\delta$ values for pyridinium protons (a) $\Delta\delta$**2a**, (b) $\Delta\delta$**4**.

Table 2. ^{13}C NMR Chemical Shifts^a of **1**−**6** and the $\Delta\delta$ Values^b (ppm)

compd	solv	δ_{C2}	δ_{C4}	δ_{C5}	δ_{C6}	$\delta_{C=X}$	$\Delta\delta_{C2}{}^b$	$\Delta\delta_{C4}{}^b$	$\Delta\delta_{C5}{}^b$	$\Delta\delta_{C6}{}^b$	$\Delta\delta_{C=X}{}^c$
1	CDCl$_3$					202.28					
1	CD$_3$CN					205.15					
1	DMSO-d_6					203.39					
2a	CDCl$_3$	147.38	143.85	127.68	144.17	204.92	4.22	−0.29	-1.05	-1.48	2.64
2a	CD$_3$CN	145.88	145.09	129.53	146.77	206.27	1.45	0.39	-0.17	0.77	1.12
2a	DMSO-d_6	144.83	144.51	128.25	146.24	204.31	1.51	0.77	-0.19	1.22	0.92
3	CDCl$_3$					153.15					
3	CD$_3$CN					154.71					
3	DMSO-d_6					152.95					
4	CDCl$_3$	146.69	144.70	127.59	145.73	153.93	3.53	0.56	-1.14	0.08	0.78
4	CD$_3$CN	146.98	145.74	129.04	146.24	154.80	1.84	-0.18	-0.66	-0.70	0.09
4	DMSO-d_6	144.66	144.98	127.70	146.25	153.33	1.34	1.24	-0.74	1.23	0.38
6a	CDCl$_3$	143.16	144.14	128.73	145.65						
6a	CD$_3$CN	144.43	145.20	129.70	146.22						
6a	DMSO-d_6	143.32	143.70	128.44	145.02						

^{a} ^{13}C NMR chemical shifts are measured at 400 MHz. ^{b} $\Delta\delta = \delta$**2a** − δ**1** or δ**4** − δ**3**. ^{c} $\Delta\delta = \delta$**1** - δ**6a** or δ**3** − δ**6a**.
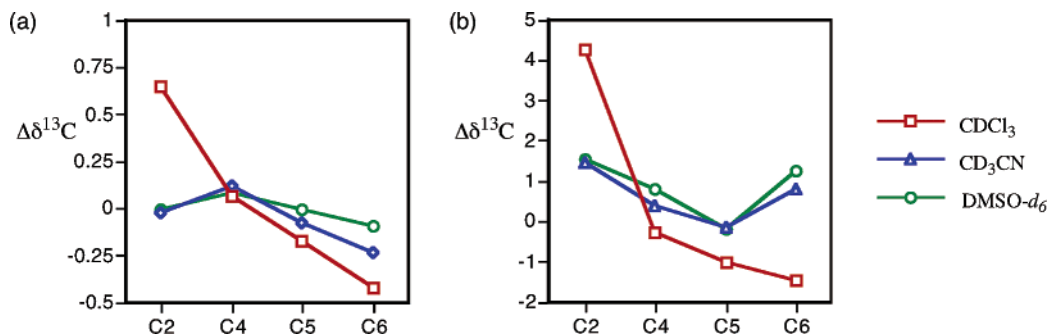

Figure 2. Plots of $\Delta\delta$ values for pyridinium carbons (a) $\Delta\delta$**2a**, (b) $\Delta\delta$**4**.

The ^{13}C NMR chemical shifts of **1**−**4** and **6a** are listed in Table 2, where nicotinic amides **1** and **3** and pyridinium salt **6a** are used as references with respect to the thiocarbonyl and the carbonyl carbons and the pyridinium carbons of **2a** and **4**, respectively. The assignments of the pyridinium carbons were performed by C−H COSY measurements. $\Delta\delta^{13}$C values are defined as the chemical shift differences from the corresponding standard **6a** similar to the $\Delta\delta^1$H values. Figure 2a,b shows plots of $\Delta\delta^{13}$C values for each carbon of **2a** and **4** in various solvents, respectively. The absolute values of $\Delta\delta_{C2}$ and $\Delta\delta_{C6}$ are larger than $\Delta\delta_{C4}$ and $\Delta\delta_{C5}$. The $\Delta\delta^{13}$C received significant solvent effect; the polar solvents decrease the $\Delta\delta$ values. These trends in $\Delta\delta_C$ are similar to those observed for $\Delta\delta_H$ values described above.

The shifts of the chemical shifts were observed not only in pyridinium carbons but also in the C=S of **2a** and the C=O of **4** in CDCl$_3$; the $\Delta\delta$**2a**$_{C=S}$ and $\Delta\delta$**4**$_{C=O}$ are 2.64 and 0.78, respectively. These carbons also receive solvent effect; the $\Delta\delta_{C=S}$ and $\Delta\delta_{C=O}$ decrease with increasing solvent polarity. The

downfield shifts of the C=X carbons may be due to the polarization of the C=X group into C$^+$−X$^-$ enhanced by the positive charge of the pyridinium ring. The larger $\Delta\delta$**2a**$_{C=S}$ than $\Delta\delta$**4**$_{C=O}$ can be explained by the larger polarizability of the C=S group than that of the C=O group.

The unusual downfield shift of H2 and C2 and upfield shift of H6 and C6 in the pyridinium ring in CDCl$_3$ would be attributable to an anisotropic effect of the C=S or the C=O group. This hypothesis is supported by X-ray structures of **2a** and **4** as described later, where the C=S and C=O groups take effective orientation for the shielding of H6 and C6 and deshielding of H2 and C2. The larger $\Delta\delta$ values in **2** compared to **4** would be the result of the larger magnetic anisotropy of a thiocarbonyl group than that of a carbonyl group.[15] Because

(14) (a) Zauhar, R. J.; Colbert, C. L.; Welsh, W. J. *Biopolymers* **2000**, *53*, 233−248. (b) Breinlinger, E. C.; Keenan, C. J.; Rotello, V. M. *J. Am. Chem. Soc.* **1998**, *120*, 8606−8609. (c) Pranata, J. *Bioorganic Chem.* **1997**, *25*, 213-219. (d) Viguera, A. R.; Serrano, L. *Biochemistry* **1995**, *34*, 8771−8779. (e) Lebl, M.; Sugg, E. E.; Hruby, V. J. *Int. J. Peptide Protein Res.* **1987**, *29*, 40−45.
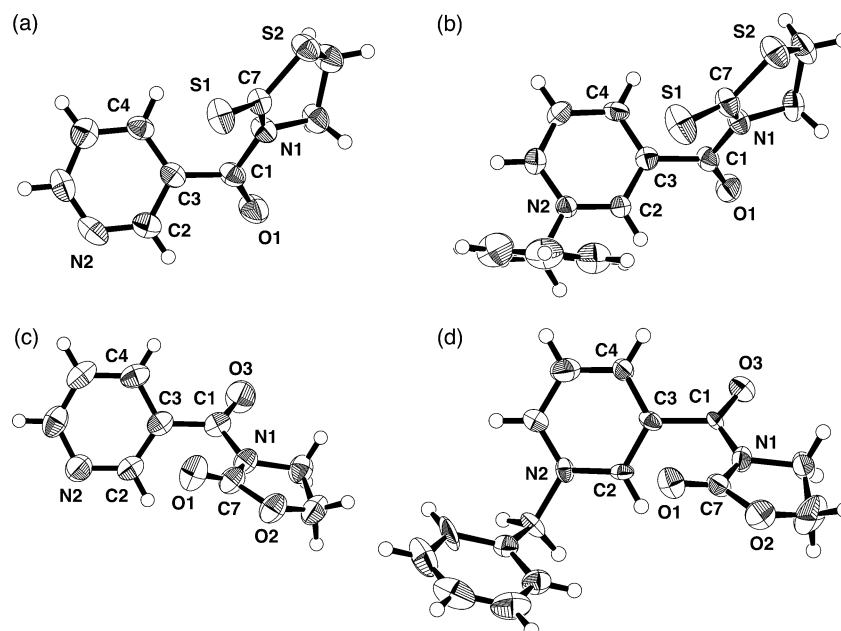
Figure 3. ORTEP drawing for (a) **1**, (b) **2a**, (c) **3**, and (d) **4** at the 30% probability level. The bromine atoms are omitted for clarity.

Table 3. $n \rightarrow \pi^*$ Bands of **1** and **2a**, and $\Delta\lambda$ Values

compd	solv.	λmax/nm (ε)	$\Delta\lambda$max/nm[a]
1	CH_3CN	409.2(190)	
1	$CHCl_3$	419.0(190)	9.8
2a	CH_3CN	421.0(270)	
2a	$CHCl_3$	424.2(630)	3.2

[a] Difference of λ values between in $CHCl_3$ and CH_3CN.

the magnitude of the anisotropic effect significantly depends on the conformational rigidity, the larger absolute $\Delta\delta$ values of **2** and **4** would arise from the highly restricted conformation caused by intramolecular interactions. The solvent effects suggest that the intramolecular interaction effectively occurs in a nonpolar solvent and is disturbed in polar solvents. These observations in ^{1}H and ^{13}C NMR studies, downfield shifts of H2 and C2, upfield shift of H6 and C6, downfield shift of C=S and C=O, and the solvent effects can be explained by the intramolecular (C=S)···Py$^+$ and (C=O)···Py$^+$interactions.

UV−Vis Spectral Studies. It is a characteristic feature of thioamides that the $n \rightarrow \pi^*$ band of the C=S group is observed at a longer wavelength region.[16] We expected that the (C=S)···Py$^+$ intramolecular interaction would affect the absorption band of the C=S group of **2a**. The $n \rightarrow \pi^*$ band of the C=S group for **1** and **2a** showed significant solvent dependence. The bands of **1** in CH_3CN and $CHCl_3$ appear at 409.2 and 419.0 nm, respectively, and those of **2a** are 421.0 and 424.2 nm, respectively (Table 3). This blue shift with increasing solvent polarity is a common feature in various thioamides[16] because polar solvents enhance the polarization of the thioamide moiety and stabilize its ground-state energy by solvation.[17] $\Delta\lambda$ Values are given in Table 3 as the differences in the wavelengths between that in CH_3CN and $CHCl_3$. An important feature is that the $\Delta\lambda$ value of **2a** is much smaller than that of **1**, meaning the ground-state energy of **2a** to be lowered even in less polar

$CHCl_3$. This stabilization can be explained by the intramolecular (C=S)···Py$^+$ interaction, which results in the shift of the $n \rightarrow \pi^*$ band into a shorter wavelength region. It should be noted that there is no CT band in both **1** and **2a**, suggesting little contribution of CT interaction into the present interaction.

X-ray Crystallographic Analyses. X-ray structural analyses of **1**, **2a**, **3**, and **4** were performed to clarify the geometrical differences among them. A list of crystal data and details of the structure determinations are given in Table 4 and their ORTEP drawings are shown in Figure 3. Since the asymmetric unit of compound **3** contains four independent molecules having similar geometries, the structure of one of four molecules is representatively indicated in Figure 3.

Thiocarbonyl or carbonyl in the five-membered ring of **1**, **2a**, **3**, and **4** each has *anti* orientation against the amide carbonyl due to the electrostatic repulsion between them, which is consistent with the reported geometries of *N*-acyl-1,3-thiazolidine-2-thiones[18] and *N*-acyl-1,3-oxazolidine-2-ones.[19] The S1 atoms of **1** and **2a** are close to C3 and C4, whereas the O1 atoms of the oxazolidinone moieties of both **3** and **4** are close to C2 and C3.

To clarify the geometrical differences, the distances between the pyridinium carbons and the S1 or O1 atom were compared. The selected interatomic distances are listed in Table 5. The S1···C3 distance of 3.051(5) Å for **2a** is significantly shorter than the sum of van der Waals radii of the sulfur and carbon atoms[20] (3.65Å). On the other hand, the S1···C3 distance of 3.211(4)Å for amide **1** is much longer than that of **2a**.[21] For oxazolidinone derivatives, the O1···C2 distance of **4** [2.820(11)Å] is shorter than that of **3** [2.982(5)Å], and is also shorter than the sum of van der Waals radii of the oxygen and carbon atoms

(15) Gribble, G. W.; Bousquet, F. P, *Tetrahedron* **1971**, *27*, 2785−3794.
(16) Walter, W.; Voss, J. In *The Chemistry of Amides*; Zabicky, J., Ed.; Wiley-interscience, London, 1970, chapter 8, pp 383−475.
(17) Berg, U.; Sandström, J. *Acta Chem. Scand.* **1966**, *20*, 689−697.

(18) (a) Yamada, S. *J. Org. Chem.* **1996**, *61*, 941−946. (b) Yamada, S. *Angew. Chem., Int. Ed. Engl.* **1993**, *32*, 1083−1085.; (c) Fujita, E.; Nagao, Y.; Seno, K.; Takao, S.; Miyasaka, T.; Kimura, M., Watson, W. H. *J. Chem. Soc., Perkin Trans. 1* **1981**, 914−919.
(19) Evans, D. A.; Ennis, M. D.; Le, T.; Mandel, N.; Mandel, G. *J. Am. Chem. Soc.* **1984**, *106*, 1154−1156.
(20) Bondi, A. *J. Phys. Chem.* **1964**, *68*, 441−451.
(21) The S···C3 distance is still shorter than the sum of van der Waals radii. This would be ascribed to its intrinsic steric demand.
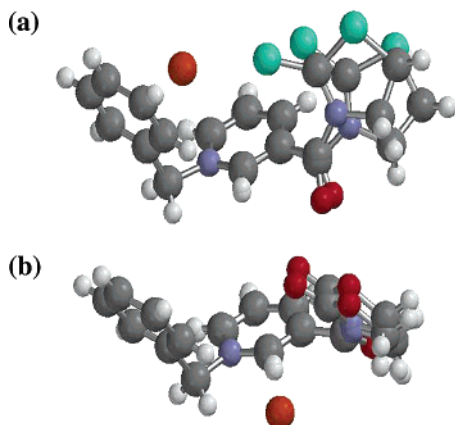
Table 4. Crystal Data and Structure Refinement for **1**, **2a**, **3**, and **4**

compd	1	2a	3	4
empirical formula	$C_9H_8N_2OS_2$	$C_{16}H_{15}BrN_2OS_2$	$C_9H_8N_2O_3$	$C_{16}H_{15}BrN_2O_3$
crystal habit, color	prismatic, yellow	prismatic, yellow	prismatic, colorless	prismatic, colorless
crystal size (mm)	$0.5 \times 0.5 \times 0.3$	$0.2 \times 0.2 \times 0.2$	$0.3 \times 0.3 \times 0.15$	$0.35 \times 0.1 \times 0.1$
formula weight	224.24	395.33	192.17	363.21
T (K)	293(2)	293(2)	293(2)	293(2)
radiation	Cu Kα, 1.54178 Å	Cu Kα, 1.54178 Å	Cu Kα, 1.54178 Å	Cu Kα, 1.54178 Å
crystal system	orthorhombic	monoclinic	monoclinic	monoclinic
space group	$P2_12_12_1$	Pn	$P2_1$	Cc
a (Å)	9.778(2)	8.132(3)	12.5019(9)	13.312(3)
b (Å)	14.647(4)	7.399(2)	24.5155(12)	9.675(3)
c (Å)	7.0557(6)	14.431(3)	5.6418(5)	14.273(3)
α (deg)	90	90	90	90
β (deg)	90	101.49(2)	89.993(7)	94.68(2)
γ (deg)	90	90	90	90
V (Å^3)	1010.5(3)	850.9(4)	1729.2(2)	1832.1(7)
Z	4	2	8	4
d calc (Mg/m^3)	1.474	1.543	1.476	1.317
abs. coefficient (mm^{-1})	3.098	5.603	0.959	3.167
theta range (deg.)	5.44 to 67.94	5.80 to 67.40	3.54 to 67.94	5.66 to 67.93
reflections collected	1977	1343	3573	1690
data/restraints/parameters	1303/0/128	1341/2/200	3232/1/506	1660/2/188
$R_1{}^a$	0.0447	0.0242	0.0342	0.0789
$wR_2{}^b$	0.1348	0.0899	0.1168	0.2189
goodness-of-fit on F^{2c}	0.800	0.976	0.778	1.183
extinction coefficient	0.24(2)	0.022(2)	0.016(2)	0.0066(13)
largest diff. peak and hole (e.A^{-3})	0.371 and −0.560	0.443 and −0.444	0.182 and −0.190	2.511 and −0.798

^{a} $R_1 = \Sigma\text{II}F_o\text{I} - \text{I}F_c\text{II}/\Sigma\text{I}F_o\text{I}$. ^{b} $wR_2 = [\Sigma[w(F_o{}^2 - F_c{}^2)^2]/\Sigma[w(F_o(F_o{}^2)^2]]^{1/2}$. ^{c} $\text{GOF} = [\Sigma[w(F_o{}^2 - F_c{}^2)^2]/\text{degrees of freedom}]^{1/2}$.

Table 5. Interatomic Distances between X (S1 or O1) with C2−C4

	$X\cdots$C2/Å	$X\cdots$C3/Å	$X\cdots$C4/Å
1	4.073(3)	3.211(3)	3.287(3)
2a	3.494(5)	3.051(5)	3.426(6)
3	2.982(5)	2.894(4)	3.767(4)
4	2.820(11)	2.896(14)	3.895(13)

Table 6. Three Parameters *a*, *b* and *c* for **1**, **2A**, **3**, and **4**

	a/Å	b/Å	d/Å
1	3.89	2.81	2.69
2a	3.53	3.04	1.80
3	3.55	2.53	2.49
4	3.55	2.34	2.67

position of the S1 atom or the O1 atom toward the pyridine or the pyridinium nucleus. Figure 4a clearly shows that the S1 atoms of **1** and **2a** occupy significantly different positions from each other; while the S1 atom of **1** is located out of the pyridine ring, the S1 atom of **2a** exists above the pyridinium plane. Figure 4b also shows that the O1 atom of **4** is closer to the pyridinium nucleus than that of **3**. These strongly suggest the existence of attractive interactions of the C=S group and the C=O group with the pyridinium ring.

The relative positions of the S1 and O1 atoms toward the pyridinium nucleus were further clarified by using three parameters *a*, *b*, and *c*, the definitions of which are as follows: *a*; distance from the centroid, *b*; vertical displacement from the pyridinium plane, *c*; horizontal displacement from the centroid. Table 6 lists the data for the three parameters of **1**−**4**. The parameters of *a* and *c* of 3.53 Å and 1.80 Å for **2a** are much smaller than those for **1** (3.89 Å and 2.69Å). This means that the S1 atom of **2a** is much closer toward the pyridinium plane than that of **1**. In the case of oxazolidinone derivatives **3** and **4**, *b* of **4** is smaller, and *c* of **4** is larger (2.34 Å and 2.67 Å, respectively) than those of **3** (2.53 Å and 2.49 Å), indicating that the O1 atom of **4** relatively exists on the side of the plane.

Figure 4. Superimposed geometries of (a) **1** and **2a** and (b) **3** and **4**.

(3.22 Å). The X-ray geometries show that the thiocarbonyl of **2a** and the carbonyl of **4** occupy effective positions for deshielding of H2 and shielding of H6. This is comparable with the unusual chemical shifts of H2 and H6 of **2a** and **4** described earlier, indicating that the geometries in both solution and in crystal are very similar.

The superimposed X-ray structures are shown in Figure 4a (**1** and **2a**) and 4b (**3** and **4**) in an effort to better understand the geometrical differences between pyridine and pyridinium derivatives.[22] The pyridine and pyridinium rings are both fixed at the same coordinate to clarify the difference in the relative

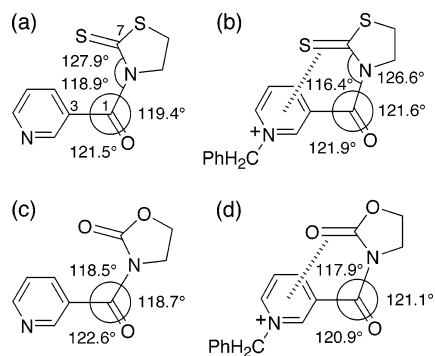(22) The graphics are drown using SPARTAN 02 (Wave function, inc.) based on X-ray geometries.

Figure 5. Bond angles around amide linkages for (a) **1**, (b) **2a**, (c) **3**, and (d) **4**.

Another important geometrical feature that supports the (C=S)···Py⁺ and the (C=O)···Py⁺ interactions is the deformation in the bond angles of **2a** and **4**. As shown in Figure 5, the N1–C1–C3 angle of 116.4(4)° for **2a** is smaller and the N1–C1–O1 angle of 121.6(4)° is larger than that of **1** [118.9(2)° and 119.4(2)°]. The corresponding general bond angles for *N*-acyl-1,3-thiazolidine-2-thiones are in the range of 119–120° and 117–118°, respectively.[18] In addition, the C1–N1–C7 angle of 126.6(4)° for **2a** is smaller than that of **1** [127.9(2)]. A similar tendency was observed for **3** and **4**; the N1–C1–O3 angle of 121.1(7)° for **4** is larger than that of **3** [118.7(3)]. All of the foregoing X-ray geometrical features of **2a** and **4**, the shorter interatomic distances of X···Py⁺ and the bond angle deformations around the amide moieties, unambiguously provide evidence for the (C=S)···Py⁺ and (C=O)···Py⁺ interactions.

It should be noted that not only was intramolecular (C=S)···Py⁺ interaction observed, but also intermolecular interaction was observed in the crystal. The X-ray packing structure for **2a** apparently shows that the sulfur atom of the thiocarbonyl group is sandwiched between the two pyridinium nuclei and the unit was in a layered arrangement (Figure 6). The S1···C6′ distance of 3.65Å is close to the sum of van der Waals radii. Interesting is that another sulfur atom S2 in the thiazolidine ring is very close to C4′ with the interatomic distance of 3.46 Å. This may be a result of the contribution of the lone pair electrons of S2 in combination with the π electron of the C=S group.

There have been known various types of interactions associated with the lone pair electrons of a heteroatom. The interaction of the lone pair electrons with a carbonyl is well-known in various systems. In particular, medium-sized cyclic aminoketones show transannular *n*···π* interaction between the amino group and the carbonyl group,[23] the N···C=O angle and the N···C distances of which are ca. 107° and 2.9–1.5 Å, respectively.[24] In addition, a partial pyramidalization in the carbonyl carbon is often observed. Recently, Frontera et al. have reported a new type of interaction between the n orbital of a heteroatom and the π* or σ* orbital of a C–C bond of an aromatic moiety.[25] They demonstrated an elongation of the C–C bond near the heteroatom in comparison with other aromatic C–C bonds. The X-ray structures of **2a** and **4** do not satisfy these geometrical
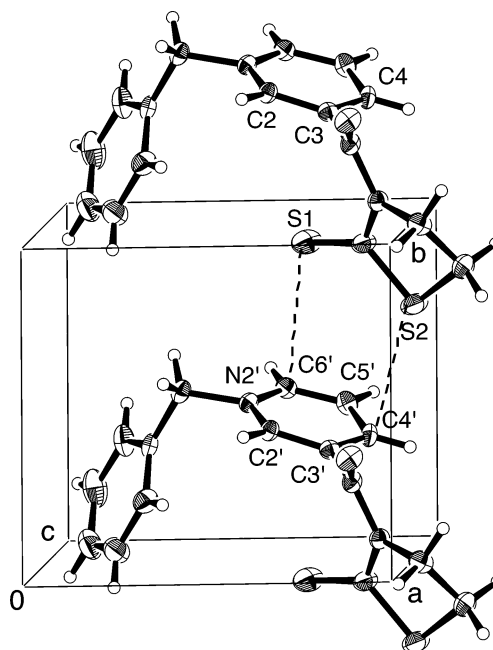
(23) (a) Birnbaum, G. I. *J. Am. Chem. Soc.* **1974**, *96*, 6165–6168. (b) Kaftory, M.; Duniz, J. D. *Acta Crystallogr.* **1975**, *B31*, 2912. (c) Kaftory, M.; Duniz, J. D. *Acta Crystallogr.* **1975**, *B31*, 2914.

(24) Bürgi, H. B.; Dunitz, J. D.; Shefter, E. *J. Am. Chem. Soc.* **1973**, *95*, 5065–5067.

(25) Qian, X.; Xu, X.; Li, Z.; Frontera, A. *Chem. Phys. Lett.* **2003**, *372*, 489–496.

Figure 6. Packing structure of **2a** and intermolecular distances. The bromine atoms are omitted for clarity.

requirements for *n*···π* or *n*···σ* interactions because the lone pair electrons of the S or O atom are not directed toward the π* or σ* orbital of the pyridinium ring. In addition, neither pyramidalization of the carbon atom nor the C–C bond elongation was detected.

There are several examples of interactions of a carbocation with a heteroatom. Asensio and co-workers have found anomalous shielding of the carbon atom of the tris(2-thienyl)methyl cation.[26] Through-space charge delocalization of the three sulfur atoms of the thiophene rings with the parallel empty p orbital has been postulated as one of explanations. Akiba and co-workers have proven a hypervalent carbocation that has trigonal pyramidal configuration with two OR groups.[27] The two neighboring OR groups occupy an apical position toward the central carbon with 2.41 and 2.43 Å of the O···C⁺ distances. Such characteristic geometrical features are not observed in the X-ray geometries of **2a** and **4**, indicating less importance of *n*···C⁺ interactions in the present cases.

Attractive S···π interaction is postulated between an aromatic ring and a divalent sulfur atom in peptides and various sulfur-containing organic compounds. This interaction is suggested on the basis of ¹H NMR studies,[14d,e] CD analyses,[14d] X-ray crystallographic analyses, theoretical studies[14d] and statistical analyses of crystallographic data of proteins,[14a] although the origin of the attractive force remains unclear. Since no such interaction is observed in **1**, the S···π interaction would not contribute to the attractive interaction in **2a**.

An intermolecular interaction of a pyridinium with a compound containing a sulfur atom has been known in several inclusion complexes. Stoddart and co-workers have reported that a tetracationic cyclophane, cyclobis(paraquat-*p*-phenylene), makes an inclusion complex with tetrathiafulvalene with a higher free energy of complexation than the other π-components, and

(26) Abarca, B.; Asensio, G.; Ballesteros, R.; Varea, T. *J. Org. Chem.* **1991**, *56*, 3224–3229.

(27) Akiba, K.-y.; Yamashita, M.; Yamamoto, Y.; Nagase, S. *J. Am. Chem. Soc.* **1999**, *121*, 10 644–10 645.
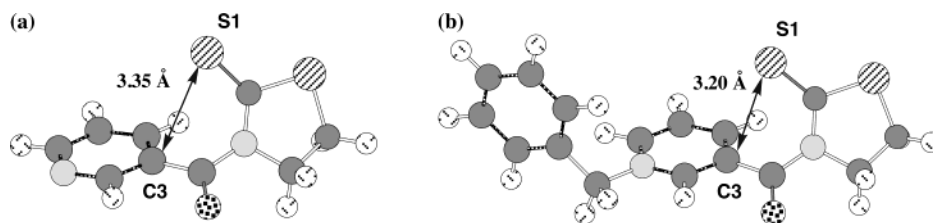
Figure 7. HF/6-311G** level optimized geometries of (a) **1** (b) **2a**.

the distance between the sulfur atom and the pyridinium ring in the complex is 3.54 Å.[28] The driving force of this complexation is explained by a charge-transfer energy, which is supported by the observation of a CT absorption band at 854 nm. Because no CT absorption band was observed in **2**, the CT interaction would be negligible in the present system.

There are only a few examples for the interactions involving participation of a thiocarbonyl group. Nagao and co-workers reported C=S···S−C interaction in some heterocyclic compounds. The origin of this interactive force is postulated to be an overlap of the *n* orbital of the S atom with the σ^*_{C-S}.

A hydrogen bonding is one important interaction that affects the conformation of the molecules and is often observed in compounds containing heteroatoms.[29] In the present cases, the C=S···H−C4 distance for **1** and **2a** are 3.219 Å and 3.800 Å, respectively, and the C=O···H−C2 distance for **3** and **4** are 2.884 Å and 2.655 Å, respectively, which are much longer than those of general hydrogen bonds. In addition, the lone pair electrons of the C=S and C=O group are not directed toward H4 and H2, respectively.

Comparison with the reported interactions involving a sulfur or an oxygen atom described above will strongly suggest that the present interactions are not consistent with reported $n \cdots \pi^*$, $n \cdots \sigma^*$, $n \cdots C^+$, $S \cdots \pi$, $S \cdots \sigma^*$, and CT interactions and the hydrogen bond. In addition, the fact that both of the C=S and the C=O groups exhibit a similar interaction with a pyridinium ring indicates the significant importance of the π electrons rather than n electrons in the present new interactions.

Ab Initio Calculations. The X-ray structures of **1** and **2a** were compared with those optimized at the HF/6-311G** level to obtain further supporting data for the intramolecular interactions. The optimized geometries shown in Figure 7 are very close to the corresponding X-ray structures. The S1···C3 distances of optimized **2a** (3.20 Å) is shorter than that of **1** (3.35 Å). This trend is comparable with their X-ray geometries, supporting the attractive interaction of the C=S group with the pyridinium ring. The similarlity between the optimized geometries and the X-ray ones suggests little crystal packing effect on the crystal structures. The longer S1···C3 interatomic distances in optimized geometries than those in X-ray geometries may be attributable to the lack of the evaluation of dispersion force in this calculation method. AIM analysis of **2a** shows that a critical point exists between the S1 and C3, whereas no critical points exist between the S1 and C3 of **1**. The AIM analysis suggests that the positively charged pyridinium nucleus enhance the interaction between the S1 and C3 in **2a**.
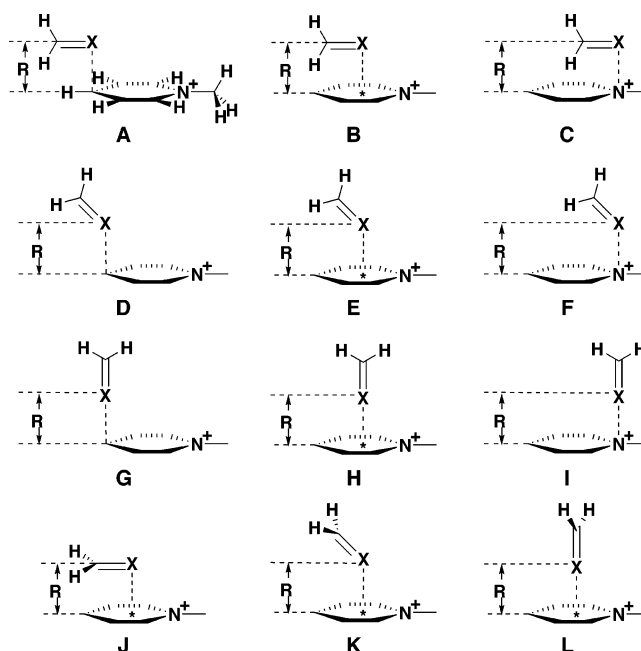
(28) (a) Balzani, V.; Credi, A.; Mattersteig, G.; Matthews, O. A.; Raymo, F. M.; Stoddart, J. F. Venturi, M.; White, A. J. P.; Williams, D. J. *J. Org. Chem.* **2000**, *65*, 1924. (b) Philp, D.; Slawin, A. M. Z.; Spencer, N.; Stoddart, J. F.; Williams, D. J. *J. Chem. Soc., Chem. Commun.* **1991**, 1584.
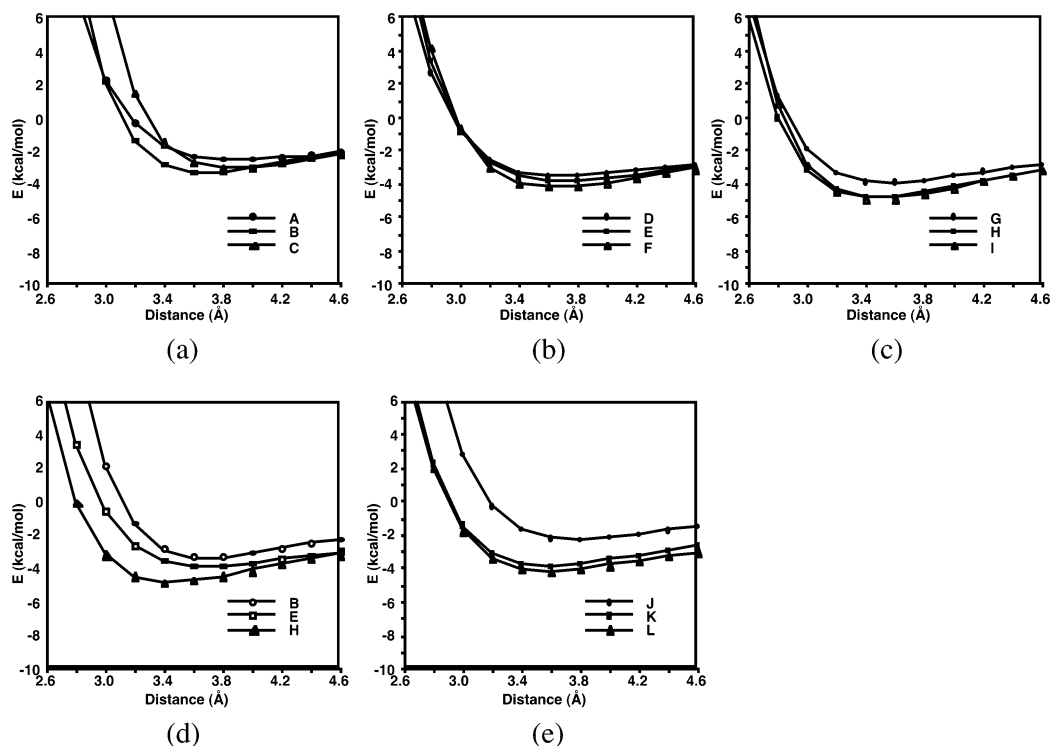(29) hydrogen bonding: Steiner, T. *Angew. Chem., Int. Ed.* **2002**, *41*, 48−76.

Figure 8. Geometries of 12 orientations of CH₂X (X=S or O) and C₅H₅-NMe⁺ complexes. * is the middle point between the nitrogen atom and the carbon atom at the para-position. The tilt angle of aldehyde is 45° in the complexes D, E, F, and K.

The MP2/6-311G** level intermolecular interaction energies of the 12 orientations of methylpyridinium and thioaldehyde complexes (Figure 8) were calculated to evaluate the orientation dependence of the (C=S)···Py⁺ interaction. The calculated interaction energies (Figure 9a−e) show that the horizontal displacement of the thioformaldehyde changes the size of the interaction energy. The complex **A** is less stable than the complexes **B** and **C**. The positive charge on the nitrogen atom would be the cause of the larger stability of the complexes **B** and **C**. The complexes **D** is also less stable than the complexes **E** and **F**, and **G** is less stable than **H** and **I**, respectively. The comparison of the complexes **B**, **E**, and **H** (Figure 9d) shows that thioformaldehyde prefers the orientation where the C=S bond is perpendicular to the ring. The complex **I** has the largest (most negative) interaction energy (−4.90 kcal/mol) at the potential minimum. The complex **L** (−4.23 kcal/mol) is slightly less stable than the complex **I**. Although the parallel orientation complex **A** (−2.60 kcal/mol) is considerably less stable than the complex **I**, the orientation of the thiocarbonyl group in **2a** is close to that in the complex **A**. The thiocarbonyl group and pyridiniym nucleus are connected by an amide bond in **2a**. Due to the short linkage the thiocarbonyl group in **2a** cannot take perpendicular orientation. Apparanetly this structural constraint is the cause of the nearly parallel orientation of the thiocarbonyl group found in **2a**.

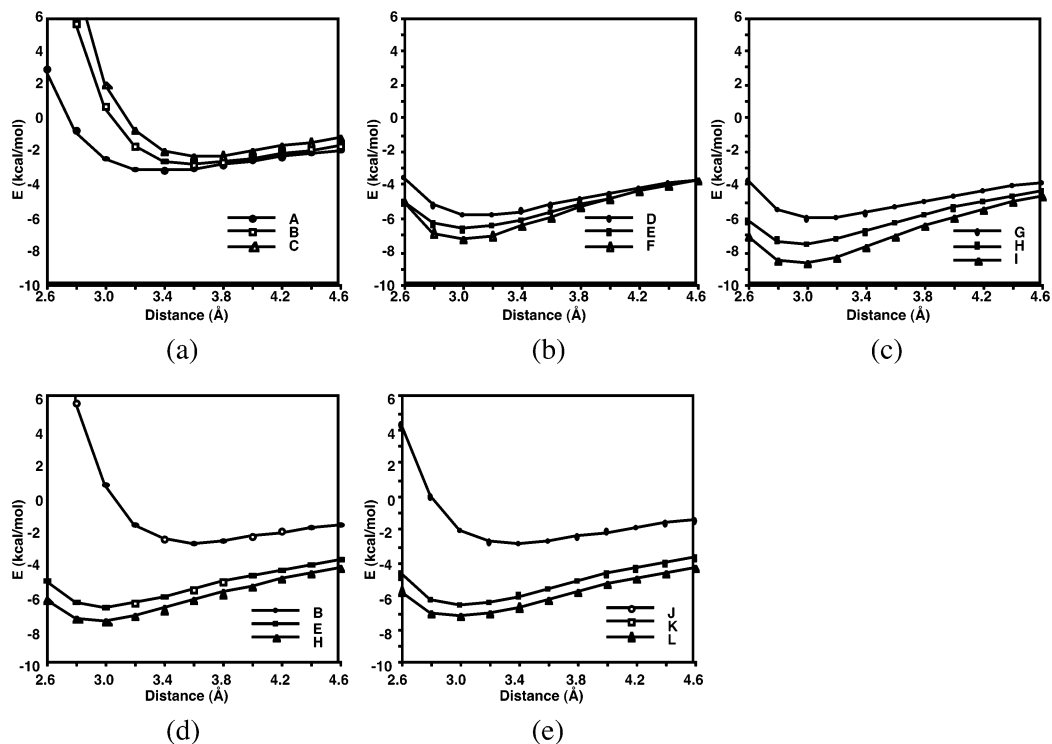**Figure 9.** Calculated interaction energies of CH₂S and C₅H₅NMe⁺ complexes at the MP2/6-311G** level.

Figure 10. Calculated interaction energies of CH₂O and C₅H₅NMe⁺ complexes at the MP2/6-311G** level.

The MP2/6-311G** level intermolecular interaction energies of the 12 orientations of methylpyridinium and formaldehyde complexes were also calculated to evaluate the (C=O)···Py⁺ interaction as summarized in Figure 10. The orientations of the complexes are the same as those of the thioaldehyde complexes shown in Figure 8. The orientation dependence of the interaction energy of the aldehyde complex is close to that of the thioaldehyde complex. The carbonyl group also prefers perpendicular orientation. The complex **I** has the largest interaction

energy (−8.75 kcal/mol) at the potential minimum as in the case of the thioaldehyde complex. The calculated interaction energy is substantially larger than that of the thioaldehyde complex (−4.90 kcal/mol). The calculated interaction energy of the complex **A** is −3.18 kcal/mol. The interaction energy of the aldehyde complex has larger orientation dependence than that of the thioaldehyde complex.

The geometries of the orientation **I** complexes were fully optimized at the MP2/6-311G** level. The optimized geometries
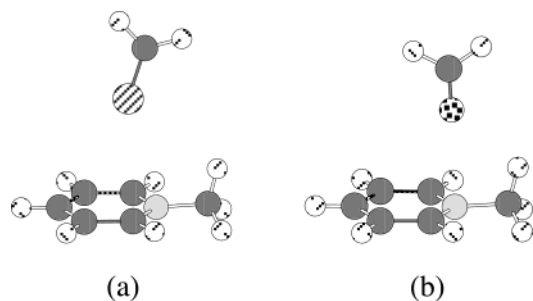
Figure 11. Optimized geometries of CH_2S (a) and CH_2O (b) complexes with $C_5H_5NMe^+$ at the MP2/6-311G** level.

have C_s symmetry (Figure 11). The optimized geometries of the thioaldehyde and aldehyde complexes show that they prefer nearly perpendicular orientation. The calculated MP2/6-311G** level interaction energies of the optimized geometries are −5.26 and −8.97 kcal/mol, respectively.

Electrostatic and induction energies of the thioaldehyde and aldehyde complexes (orientation **A**) were calculated to elucidate the origin of the (C=S)···Py$^+$ and (C=O)···Py$^+$ interactions. Figure 12 shows the calculated interaction energy profiles of the model systems. R is the distance between the C4 and the S or the O atom. The total interaction energy (E_{MP2}) was calculated at the MP2/6-311G** level. The E_{es} and E_{ind} are the electrostatic and induction energies, respectively. E_{corr} ($= E_{MP2} − E_{HF}$) is the contribution of electron correlation to the calculated interaction energy, which is mainly dispersion energy. E_{rep} ($= E_{HF} − E_{es} − E_{ind}$) is mainly exchange-repulsion energy, but it also includes other terms. The E_{MP2} values of the two model systems (HCHS···$C_5H_5NMe^+$ and HCHO···$C_5H_5NMe^+$) at the potential minima are −2.60 kcal/mol ($R = 4.0$ Å) and −3.18 kcal/mol ($R = 3.4$ Å), respectively. The potential energy curves of E_{MP2} indicate that substantial attraction still exists even when the molecules are well separated ($R > 5.0$ Å), which shows that the major source of the attraction in these systems are long-range interactions such as induction and electrostatic interactions.

Indeed, the major contributors for the attraction are E_{es} and E_{ind} values as shown in Figure 12. It has been reported that electrostatic interaction is the major source of the attraction in cation−π interaction.[30] Moreover, one of the authors reported that induction is also important for the attraction in cation−π interaction.[31] Therefore, the present (C=S)···Py$^+$ and (C=O)···Py$^+$ interactions are grouped into a cation−π interaction, though the interactive energies are much smaller than aromatic−π and metal−cation interactions.[1c] The solvent effects observed in NMR experiments, where the interaction is stronger in a nonpolar solvent, are in agreement with the predicted relationship of dielectric constants with the cation−π interaction energies.[32]

The interaction energies of the model systems shown in Figure 13 were calculated to estimate the contributions of electrostatic and induction energies to the (C=S)···Py$^+$ and (C=O)···Py$^+$ interactions in **2** and **4**. The positions of heavy atoms of the model systems were taken from the X-ray structures, while the positions of hydrogen atoms were optimized at the HF/6-311G** level. The hydrogen atoms of HCHO and

HCHS were kept within the N−C=S or N−C=O plane during the optimizations. The calculated E_{es} and E_{ind} for the model of **2** are −0.40 and −1.92 kcal/mol, and those of **4** are −0.59 and −1.53 kcal/mol, respectively, suggesting the significant importance of E_{ind} in these systems.

The larger contribution of E_{ind} of **2** into E_{MP2} than that of **4** will be owing to facile polarizability of the C=S group than the C=O group. On the other hand, the relatively larger contribution of E_{es} of **4** than that of **2** would be due to stronger electronegativity of the O atom than that of the S atom, which may result in close contact with the most electron positive C2 atom.

Recently, several examples of a new type of attractive interaction of an electron deficient aromatic ring with an electronegative atom have been reported.[33,34] Theoretical studies predicted the existence of an anion−π interaction[33] between C_6F_6 and an anion such as H$^−$, F$^−$, Cl$^−$, and Br$^−$. Similar interactions between C_6F_6 and electronegative atoms have also been elucidated.[34] These interactions seem to be closely related to the present (C=S)···Py$^+$ and (C=O)···Py$^+$ interactions because the E_{es} and E_{ind} are major contributors in both interactive energies. Since in the present systems any anion does not participate in the interactions,[35] the present interactions should be formally categorized into a cation−π interaction. Although the larger contribution of the lone pair electrons of electronegative heteroatoms into E_{es} has been reported,[34] the contribution of the lone pair electrons of the C=X groups on the attractive interaction still remain unclear. However, the $\Delta\delta_{C=S}$ and $\Delta\delta_{C=O}$ values in ^{13}C NMR studies strongly suggest the polarization of the π-electrons of the C=S and C=O groups. In addition, the prediction that E_{ind} is larger than E_{es} in the model systems as described above (Figure 13) suggest the significant contribution of the π-electrons on the present (C=S)···Py$^+$ and (C=O)···Py$^+$ interactions.

Conclusion

^{1}H and ^{13}C NMR studies, X-ray crystallographic analyses, UV−vis spectral studies and ab initio calculations provided evidence for the new attractive interactions between a thiocarbonyl group and a pyridinium ring and between a carbonyl group and a pyridinium ring. The NMR studies proved that the relative positions of the C=X group and the pyridinium ring are significantly restricted in CDCl$_3$. The X-ray analysis clarified the close contact of the C=X group and the pyridinium ring with deformation in the bond angles around the amide moieties. The blue shift in $n\rightarrow\pi^*$ absorption of **2a** suggests the stabilization of the ground-state energy in CHCl$_3$. Optimized geometries of **1** and **2a** by ab initio calculations were very close to the corresponding X-ray structures. The facts that the present interactions are inconsistent with the reported $n\cdots\pi^*$, $n\cdots\sigma^*$, $n\cdots C^+$, $S\cdots\pi$, and CT interactions and the hydrogen bonds where n electrons play a key role suggest the importance of the

(30) E.; Luque, F. J.; Orozco, M. *Proc. Natl. Acad. Sci. U.S.A.* **1998**, *95*, 5976−5980.
(31) Tsuzuki, S.; Yoshida, M.; Uchimaru, T.; Mikami, M. *J. Phys. Chem.* A **2001**, *105*, 769−773.
(32) Gallivan, J. P.; Dougherty, D. A. *J. Am. Chem. Soc.* **2000**, *122*, 870−874.

(33) Quiñonero, D.; Garau, C.; Rotger, C.; Frontera, A.; Ballester, P.; Costa, A.; Deyà, P. M. *Angew. Chem., Int. Ed.* **2002**, *41*, 3389−3392.
(34) (a) Alkorta, I.; Rozas, I.; Elguero, J. *J. Org. Chem.* **1997**, *62*, 4687−4691. (b) Gallivan, J. P.; Dougherty, D. A. *Org. Lett.* **1999**, *1*, 103−106. (c) Danten, Y.; Tassaing, T.; Besnard, M. *J. Phys. Chem. A* **1999**, *103*, 3530−3534.
(35) The bromide ion of the pyridinium salt is significantly apart from the pyridinium ring. The X-ray structure shows that the bromide ion of **2a** is located on the side of the pyridinium ring, and the distance of Br$^−$···Py$^+$ (4.772 Å) is much longer than that of reported Br$^−$···C_6F_6 (3.214 Å), suggesting little effect of the bromide ion in this interaction.
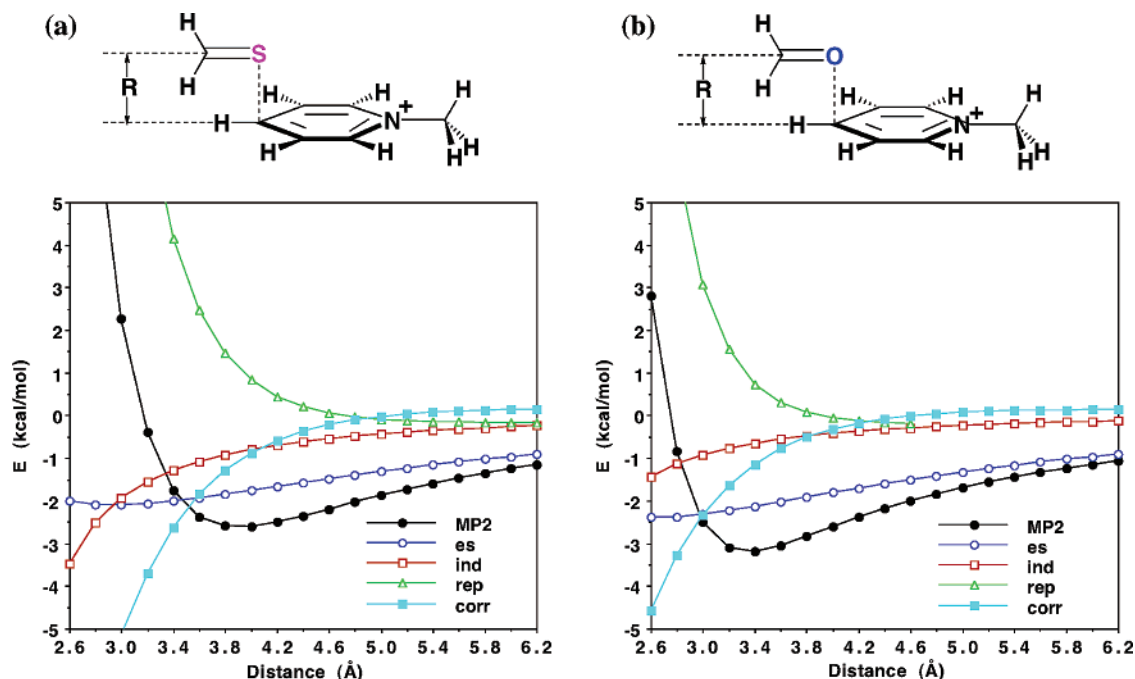
Figure 12. Interaction energy of the complexes between (a) CH_2S and $C_5H_5NMe^+$ and (b) CH_2O and $C_5H_5NMe^+$.

(a) E_{es} = -0.40 (kcal/mol)
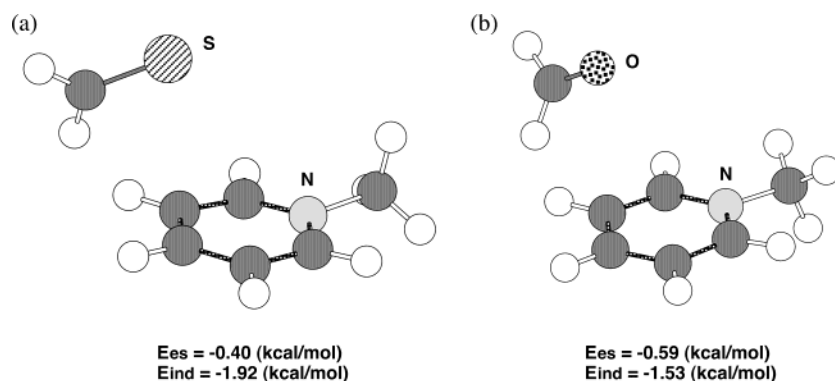E_{ind} = -1.92 (kcal/mol)

(b) E_{es} = -0.59 (kcal/mol)
E_{ind} = -1.53 (kcal/mol)

Figure 13. Calculated interaction energies of models for (a) **2** and (b) **4**.

π electrons of the C=S and the C=O groups in these interactions. Optimized geometries of the model complexes of thioformaldehyde and formaldehyde with *N*-methylpyridinium show that they prefer nearly perpendicular orientation with the interaction energies of −5.26 and −8.97 kcal/mol, respectively. The ab initio calculations for the model systems of the pyridinium salts **2** and **4** predicted the significant contribution of E_{ind} and E_{es}, which lead to a conclusion that these new attractive interactions would be grouped into a cation-π interaction.

Experimental Section

General. ^1H and ^{13}C NMR measurements were performed in 20 mmol/L solution of $CDCl_3$, CD_3CN, or DMSO-d_6 at room temperature with a JEOL JNM-GX 270 or JNM-GSX 400 spectrometer. Chemical shifts (δ) are given in ppm downfield from tetramethylsilane as the internal standard; *J*-values are given in hertz (Hz). IR spectra were obtained on a Perkin Elmer FT-IR spectrometer SPECTRUM 2000; Peaks are reported in cm^{-1}. UV–vis spectra were recorded on a SHIMADZU UV-2200 spectrophotometer in a 1-cm quartz cell in CH_3CN or $CHCl_3$. EI-MS spectra (70 eV) were recorded with a JEOL MStation JMS-700 mass spectroscopy. Analytical thin-layer chromatography (TLC) was performed on Merck thin layer 60 F254 plates.

Preparation of 1-Methyl-3-(2-thioxo-1,3-thiazolidine-3-carbonyl) Pyridinium Bromide (2b). To a solution of **1** (620 mg, 2.77 mmol) in dry CH_2Cl_2 (10 mL) was added BnBr (430 μL, 3.62 mmol), and the solution was stirred for 16 h at 50 °C. Concentration of the reaction mixutre yielded precipitates, which were filtered to give **2b** in 85% yield as yellow crystals (933 mg, 2.36 mmol); mp 187−188 °C; IR (KBr) 2943, 1709, 1330, 1241, 1180, 1151, 1057 cm^{-1}; ^1H NMR (400 MHz, $CDCl_3$) δ 10.73 (1H, s), 8.71 (1H, d, *J* = 5.2 Hz), 8.57 (1H, d, *J* = 7.6 Hz), 7.99 (1H, t, *J* = 6.8 Hz), 4.72 (2H, t, *J* = 7.6 Hz), 4.64 (3H, s), 3.89 (2H, t, *J* = 7.6 Hz); MS m/z 224 (M^+ − 94, 59%), 69 (100), 79 (15), 106, (89), 119 (80); HRMS calcd for $C_9H_8N_2OS_2$ (M^+ − 94) 224.0044, found 224.0067.

Computational Method

The Gaussian 98 program[36] was used for ab initio molecular orbital calculations. The 6-311G** basis set[37] was used for the calculations. Electron correlation correction was accounted for at the MP2 level.[38,39] The geometries of **1** and **2a** were optimized using the gradient optimization routine in the program. Harmonic vibrational frequencies were evaluated using the vibrational normal-mode analysis routine of the program to confirm the minimum nature of the structures. The basis set superposition error (BSSE)[40] was corrected using the counterpoise method.[41] Atoms in molecules (AIM) analysis of the optimized

structures was carried out using the MP2/6-311G** wave functions with the analysis routine in the program.[40] Distributed multipoles[43,44] up to hexadecapole on all atoms were obtained from the MP2/6-311G** wave functions of an isolated molecule using CADPAC version 6.[45] The electrostatic and induction energies of the complexes were calculated by using Orient version 3.2.[46] The electrostatic energies of the complexes were calculated as interactions between distributed multipoles of monomers. The induction energies were calculated as interactions of polarizable sites with electric field produced by the multipoles of monomers.[47] The atomic polarizabilities of carbon (α = 10 au), nitrogen (α = 8 au), oxygen (α = 6 au) and sulfur (α = 20 au) were used for the calculations.[48] Distributed multipoles and polarizabilities were used only for the estimation of the electrostatic and induction energies.

Supporting Information Available: The optimized geometries and calculated energies (Tables S1−S6) and CIF data for complexes mentioned in this work. This material is available free of charge via the Internet at http://pubs.acs.org.

JA0490119

(36) Frisch, M. J.; Trucks, G. W.; Schlegel, H. B.; Scuseria, G. E.; Robb, M. A.; Cheeseman, J. R.; Zakrzewski, V. G.; Montgomery, J. A. Jr.; Stratmann, R. E.; Burant, J. C.; Dapprich, S.; Millam, J. M.; Daniels, A. D.; Kudin, K. N.; Strain, M. C.; Farkas, O.; Tomasi, J.; Barone, V.; Cossi, M.; Cammi, R.; Mennucci, B.; Pomelli, C.; Adamo, C.; Clifford, S.; Ochterski, J.; Petersson, G. A.; Ayala, P. Y.; Cui, Q.; Morokuma, K.; Malick, D. K.; Rabuck, A. D.; Raghavachari, K.; Foresman, J. B.; Cioslowski, J.; Ortiz, J. V.; Stefanov, B. B.; Liu, G.; Liashenko, A.; Piskorz, P.; Komaromi, I.; Gomperts, R.; Martin, R. L.; Fox, D. J.; Keith, T.; Al-Laham, M. A.; C. Peng, Y.; Nanayakkara, A.; Gonzalez, C.; Challacombe, M.; Gill, P. M. W.; Johnson, B.; Chen, W.; Wong, M. W.; Andres, J. L.; Gonzalez, C.; Head-Gordon, M.; Replogle, E. S.; Pople, J. A. *Gaussian 98;* Gaussian, Inc.: Pittsburgh, PA, 1998.
(37) Krishnan, R.; Binkley, J. S.; Seeger, R.; Pople, J. A. *J. Chem. Phys.* **1980,** *72,* 650.
(38) Møller, C.; Plesset, M. S. *Phys. Rev.* **1934**, *46*, 618.
(39) Head-Gordon, M.; Pople, J. A.; Frisch, M. J. *Chem. Phys. Lett.* **1988**, *153*, 503.
(40) Dewar, M. J. S.; Zoebisch, E. G.; Healy, E. F. *J. Am. Chem. Soc.* **1985,** *107,* 3902.
(41) Ransil, B. J. *J. Chem. Phys.* **1961,** *34,* 2109.
(42) Boys, S. F.; Bernardi, F. *Mol. Phys.* **1970,** *19,* 553.
(43) Stone, A. J.; Alderton, M. *Mol. Phys.* **1985,** *56,* 1047.

(44) Stone, A. J. *The Theory of Intermolecular Forces*; Clarendon Press: Oxford, 1996.
(45) Amos, R. D.*CADPAC: The Cambridge Analytical Derivatives Package, Issue 6,* Technol. rep., University of Cambridge, 1995, A suite of quantum chemistry programs developed by Amos, R. D. with contributions from Alberts, I. L.; Andrews, J. S.; Colwell, S. M.; Handy, N. C.; Jayatilaka, D.; Knowles, P. J.; Kobayashi, R.; Laidig, K. E.; Laming, G.; Lee, A. M.; Maslen, P. E.; Murray, C. W.; Rice, J. E.; Simandiras, E. D.; Stone, A. J.; Su, M. D.; Tozer, D. J.
(46) Stone, A. J.; Dullweber, A.; Hodges, M. P.; Popelier, P. L. A.; Wales, D. J. *Orient: a program for studying interactions between molecules version 3.2.* University of Cambridge, 1995.
(47) Stone, A. J. *Mol. Phys.* **1985,** *56,* 1065.
(48) van Duijnen, P. T.; Swart, M. *J. Phys. Chem. A* **1998,** *102,* 2399.